Wireless Engineering and Technology, 2012, 3, 152-159
http://dx.doi.org/10.4236/wet.2012.33022 Published Online July 2012 (http://www.SciRP.org/journal/wet)

Design and Modeling of Electromagnetic Impedance Surfaces to Reduce Coupling between Antennas

Yong S. Joe[1], Jean-François D. Essiben[2], Jangsik Cho[1,3], Eric R. Hedin[1]

[1]Center for Computational Nanosciences, Department of Physics and Astronomy, Ball State University, Muncie, USA; [2]Department of Electrical Engineering, Advanced Teachers' Training College for Technical Education, University of Douala, Douala, Cameroon; [3]Department of Informational Statistics, Kyungsung University, Busan, Korea.
Email: ysjoe@bsu.edu

Received March 22nd, 2012; revised April 18th, 2012; accepted April 26th, 2012

ABSTRACT

We study the coupling problem of two waveguide antennas using the design of a two-dimensional inhomogeneous impedance structure with a fixed reflected field. Since this structure enables electromagnetic compatibility between antennas located on a plane, the behaviors of the electromagnetic field along the impedance structure are investigated. The method of moments is used to solve the integral equations and the numerical results are presented and analyzed. To reduce coupling between antennas, we need to take into account both the amplitude distribution of the field along the structure and in the openings of the antennas. In addition, while designing the structure, it is necessary to control the coefficient of decoupling.

Keywords: Coupling; Waveguide; Impedance Structure; Electromagnetic Compatibility

1. Introduction

During last decade, the process of development of radio electronics, radio location, radio navigation, and radio communication worldwide was characterized by the following basic tendencies: technical realization of enhanced physical effects and technical solutions, aspiration to accomplish transmission and information processing in real time with the broad use of computers, and the expansion of the applications solved by technology. As a consequence, despite micro-miniaturization of radio electronics facilities (REF), the volume occupied by such equipment on mobile and stationary objects is increasing [1,2]. The progression of these modern trends is vitally necessary, but it aggravates even more the serious problem of the provision in radio engineering complexes (REC) of *electromagnetic compatibility*, which is understood as the ability of REF and REC to function together with limited degradation of their own essential parameters and features.

Practically, it is often required to provide significant decoupling between the receiving and transmitting antennas, located on a common surface at a small distance from each other. One of the most well-known ways to reduce coupling between antennas is the application of electromagnetic bandgap (EBG) structures [3-8]. The EBG structures have received increased attention in recent years [9] in the areas of the microwave application. For example, a corrugated metal surface may be viewed as a structure consisting of infinitely many identical cavities, each having an aperture that is open to the air half-space. The EBG property emerges by virtue of periodic reactive loading of the guiding structure. As shown in papers [10-13], the most effective solution to the problem of providing minimum coupling between antennas is to present and resolve inverse problems of electrodynamics.

In this paper, we re-visit the bandgap structure and present another interesting mathematical model for designing the structure and suppressing surface waves on metals. In addition, we examine the possibility of reducing the coupling between antennas located on the plane, using an inhomogeneous synthesized impedance. In particular, we investigate the design problem of the impedance surface when an infinite thread of in-phase magnetic current is located above the plane at a certain height, and also the case with its location right on the impedance surface. Finally, the behaviors of the complete field on the impedance surface and the decoupling level between antennas are also investigated.

The paper is organized as follows: in Section 2, we consider a solution to the problem of synthesis of an inhomogeneous impedance plane by a fixed reflected field.

A solution to the problem of coupling of antennas on an impedance plane is given in Section 3, and numerical results are discussed in Section 4. Finally, Section 5 is devoted to conclusions.

2. Design of Impedance Surface

2.1. Statement of the Design Problem

First, we consider a solution to the two-dimensional design problem for the arrangement shown in **Figure 1**. Above the plane $S(y=0)$, there is an infinite thread of in-phase magnetic current $\boldsymbol{J}^{m\cdot ex.}$ located at the height h. On the surface S, the boundary impedance conditions of Shukin-Leontovich are fulfilled:

$$\mathbf{n}\times\mathbf{E}=-Z\mathbf{n}\times(\mathbf{n}\times\mathbf{H}), \tag{1}$$

where $\mathbf{n}=-\mathbf{i}_y$ is the unit normal to the $y=0$ plane, Z is the surface impedance, $\mathbf{E}$ is the electric field, and $\mathbf{H}$ is the magnetic field.

It is necessary to determine the dependence of the passive impedance $Z(x)(\mathrm{Re}(Z)\geq 0)$ on the surface S. Once $Z(x)$ is obtained, the complete field in the upper space is found, and then the degree of decoupling between antennas can be obtained.

2.2. Solution of the Design Problem

To obtain a solution to the problem, we introduce an orthogonal coordinate system in such a way that the plane $x0z$ coincides with the impedance plane. Then, axis $0z$ is directed parallel with the thread of the current, as shown in **Figure 1**. Further, we present the fields $\mathbf{E}$ and $\mathbf{H}$ on the surface as a sum of the incident and the reflected fields, respectively;

$$\begin{Bmatrix}\mathbf{E}\\ \mathbf{H}\end{Bmatrix}=\begin{Bmatrix}E_x^i+E_x^r\\ H_z^i+H_z^r\end{Bmatrix}, \tag{2}$$

where E_x^r and H_z^r are reflected fields, $H_z^i=H_0^{(2)}(kR_i)$, and $E_x^i=-iW\cos\gamma_i H_1^{(2)}(kR_i)$. Here, $H_0^{(2)}$ is the zeroth-order Hankel function of the second kind, $k=2\pi/\lambda$ is the wave number, λ is the wavelength, i is the imaginary unit, $W=120\pi(ohms)$ is the characteristic resistance of free space, $\cos\gamma_i=h/R_i$, and $H_1^{(2)}$ is the first order Hankel function of the second kind.

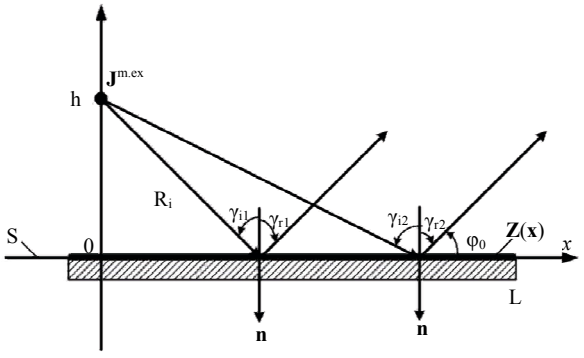

Figure 1. Geometry of the design problem. The magnetic current $J^{m\cdot ex}$ is located at the height h.

The reflected field can be written as a sum of the reflected field (E_x^{r0},H_z^{r0}) in the fixed horizontal direction and the mirror-image field (E_x^{rz},H_z^{rz}) with unknown amplitude [13]:

$$E_x^r=E_x^{r0}+E_x^{rz}\quad\text{and}\quad H_z^r=H_z^{r0}+H_z^{rz},$$

where E_x^{rz} and H_z^{rz} are field vector components of an imaginary mirror source, E_x^{r0} and H_z^{r0} are field vector components of the given reflected fields. The solution to the design problem given in this paper differs from the solution in [13] by the fact that there is no supposition of a large value of the distance $(R_i=\sqrt{h^2+x^2})$, since the solution of reducing coupling between antennas in close proximity is of primary importance. The sense of this representation will become clear with further observation.

We now consider the analytical presentation of the distributed field on the $y=0$ plane. As long as the amplitude of the plane wave does not vary along the direction of its distribution, then for the reflected field in the direction $\varphi=\varphi_0$, it is possible to write:

$$H_z^{r0}=H^{r0}H_r(x)e^{-ik(x\cos\varphi_0+y\sin\varphi_0)}, \tag{3}$$

where $H_r(x)=H_z^i e^{ikR_i}$ is the distribution of the scattered field on the surface $y=0$. We represent the mirror-image field on the impedance plane as the following way:

$$H_z^{rz}=H^z H_z^i,$$

where H^z is the constant amplitude. Then, the summative magnetic field on the surface $y=0$ can be written

$$H_z=H_z^i\left(1+H^z+H_r(x)\cdot e^{i\chi}\right), \tag{4}$$

where $\chi=k(R_i-x\cos\varphi_0)$. From the first Maxwell equation, neglecting the derivative multiplier $H_r(x)$ and H^z, we obtain for E_x normalized on W:

$$\begin{aligned}E_x=&-i(1-H^z)\cos\gamma_i H_1^{(2)}(kR_i)\\&+\left\{H_r\left[i\sin\gamma_i H_1^{(2)}(kR_i)+(\sin\gamma_i-\sin\varphi_0)H_0^{(2)}(kR_i)\right]\right.\\&\left.-\tan\varphi_0 H_r' H_0^{(2)}(kR_i)\right\}e^{i\chi},\end{aligned} \tag{5}$$

where $H_r'=\dfrac{\partial H_r(x)}{ik\partial x}$. As a result, for the required impedance normalized on W, we also have:

$$\begin{aligned}Z(x)=&\left\{-(1-H^z)\cos\gamma_i T(kR_i)\right.\\&+H_r\left[\sin\gamma_i(1+T(kR_i))-\sin\varphi_0\right]e^{i\chi}\\&\left.-\operatorname{cotan}\varphi_0 H_r' e^{i\chi}\right\}\Big/\left(1+H^z+H_r(x)\cdot e^{i\chi}\right),\end{aligned} \tag{6}$$

where $T(kR_i) = i\dfrac{H_1^{(2)}(kR_i)}{H_0^{(2)}(kR_i)}$ and $\sin\gamma_i = \dfrac{x}{R_i}$. In the general case, the resulting correlation gives the dependence of the passive impedance which gives a real part that can acquire positive as well as negative values.

Next, let us consider the design problem of the purely reactive impedance $(\mathrm{Re}(Z) = 0)$. Presenting the correlation of Equation (6) as a real and imaginary part, we can obtain the condition of feasibility of purely reactive impedance:

$$\begin{aligned}&\mathrm{Re}\left\{-\left(1-H^z\right)\cos\gamma_i T + H_r\left[\sin\gamma_i\left(1+T\right)-\sin\varphi_0\right]e^{i\chi}\right.\\&\left.-\mathrm{cotan}\phi_0 H_r' e^{i\chi}\right\}\times\left(1+H^z+H_r e^{-i\chi}\right)=0.\end{aligned} \tag{7}$$

An additional degree of freedom in the form of a mirror-image field H^z gives an opportunity to realize the impedance structure with $H_r(x) = const$ [13]. In this case, it is possible to find the impedance in the elegant form:

$$Z = -iW\cos\gamma_r\tan\frac{\chi}{2}, \tag{8}$$

where $\cos\gamma_r = \sin\varphi_0$ and γ_r is an angle of reflection. When the source of the field in Equation (6) is located right on the impedance surface $(h = 0\ (\cos\gamma_i = 0))$, which provides a completely normal (at the angle $\varphi_0 = 90^\circ$) reflection of the incident wave (without a mirror-image, $H^z = 0$), the required impedance can be expressed:

$$Z(x) = \frac{H_r(x)T(kR_i)e^{i\chi}}{1+H_r(x)\cdot e^{i\chi}}, \tag{9}$$

where $\chi = k|x|$ and $R_i = |x|$. From the condition of purely reactive impedance feasibility

$$\mathrm{Re}\left\{H_r T e^{i\chi}\left(1+H_r e^{-i\chi}\right)\right\} = 0,$$

it is not difficult to find the variation of the wave reflected from the inhomogeneous impedance plane, H_r:

$$H_r = \frac{T''}{T'}\sin\chi - \cos\chi, \tag{10}$$

where $T = T' + iT''$. In this case, the impedance can also be found from a straightforward expression:

$$Z = iT'\left(\frac{T''}{T'} - \mathrm{cotan}\chi\right) = i\left(T'' - T'\mathrm{cotan}\chi\right), \tag{11}$$

where $\dfrac{T''}{T'} = \dfrac{J_0(k|x|)J_1(k|x|)+N_0(k|x|)N_1(k|x|)}{J_0(k|x|)N_1(k|x|)-N_0(k|x|)J_1(k|x|)}$, J_0 and J_1 are the zeroth and first-order Bessel functions, respectively, and N_0 and N_1 are the zeroth and first-order Neumann functions, respectively.

3. Model Analysis

The fact that variation of the surface impedance causes radiation of energy can be used to increase the decoupling between antennas, as well as to reduce the backscattering of the antennas. An example of a similar application of the surface impedance appears in **Figure 2**. Here, the resulting surface impedances change sharply, which brings about considerable decrease in current (because of re-radiation and reflection) flowing beyond the edge of the aperture or arriving at the second antenna.

The general system studied in this section has two aperture antennas in the shape of the open ends of parallel-plate waveguides (transmitting and receiving ones) with opening sizes of *a* and *b*, which are located on the *y* = 0 plane at a distance *L* from each other. On the *y* = 0 plane, several boundary conditions of Shukin-Leontovich [Equation (1)] are fulfilled. To solve the problem of analysis, we use the Lorentz lemma in the integral form for each of the three areas: V_1, V_2, and V_3, shown in **Figure 2**, *i.e.*, by defining the field excited in the upper half-space (region V_1), the radiating waveguide (region V_2), and the receiving (region V_3) waveguide [14]. Then we can obtain a system of integral equations relative to the unknown tangential components of the electric field on the surface ($x \in [a+L+b]$ and $y = 0$) by taking into account the boundary conditions on the surface of the impedance flanges and the equality of the tangential field components in the openings of the waveguides ($H_{z1} = H_{z2}, E_{x1} = E_{x2}$ in $x \in [0, a]$; $H_{z1} = H_{z3}, E_{x1} = E_{x3}$ in $x \in [a+L, a+L+b]$):

$$\begin{cases}\displaystyle\int_0^a E_x(x')\left[H_{z1}^m(x,x') + H_{z2}^m(x,x')\right]\mathrm{d}x' + \int_a^{a+L+b} E_x(x')H_{z1}^m(x,x')\,\mathrm{d}x' = 2H_0 & x \in [0,a]\\ E_x(x) - Z(x)\displaystyle\int_0^{a+L+b} E_x(x')H_{z1}^m(x,x')\,\mathrm{d}x' = 0 & x \in [a, a+L]\\ \displaystyle\int_0^{a+L} E_x(x')H_{z1}^m(x,x')\,\mathrm{d}x' + \int_{a+L}^{a+L+b} E_x(x')\left[H_{z1}^m(x,x') + H_{z3}^m(x,x')\right]\mathrm{d}x' = 0 & x \in [a+L, a+L+b]\end{cases} \tag{12}$$

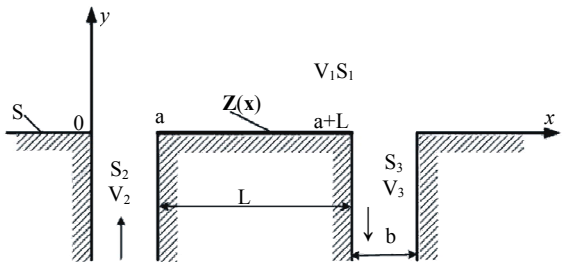

Figure 2. The general system studied has two aperture antennas in the shape of the open ends of parallel-plate waveguides (transmitting and receiving ones) with opening sizes of *a* and *b*, which are located on the *y* = 0 plane at a distance *L* from each other. The system is composed of three regions: V_1, V_2, and V_3.

where the subsidiary magnetic fields $H_{z1}^{m}(x,x')$, $H_{z2}^{m}(x,x')$, and $H_{z3}^{m}(x,x')$ are solutions of the non-uniform Helmholtz equations for complex amplitudes of the vector potentials for regions V_1, V_2, and V_3, respectively. In this way, the fields in the opening of the antennas and on the impedance part of the flange can be found. From this, the minimum level of coupling between the two antennas can then be determined.

It is necessary to note that development of an algorithm for the mathematical model under consideration is based on the specifics of the electric field at the edges $(x=0,\ a;\ a+L;\ a+L+b)$ and on the numerical solution of a system of integral equations through the Krylov-Bogolyubov method [15].

4. Results and Discussion

From remarks made earlier, the synthesized impedance structure must provide the decoupling of aperture antennas located on the same plane. The height of such antennas above the plane equals zero. In practice, the problem of synthesis is solved in the absence of the second antenna.

We next study the behavior of the complete field $H_z(x)$ on the impedance surface as a function of its dimensions and the parameters, h and φ_0. In **Figure 3**, we show a graph of the variation of the impedance distribution [Equation (8)] with the following parameters: $h=0.5\lambda$ and $\varphi_0=30^\circ$ (solid line), $\varphi_0=45^\circ$ (dashed line), $\varphi_0=60^\circ$ (dotted line). We see in **Figure 3** that the impedance distribution which gives a nearly hyperbolic reactance is the one for the angle $\varphi_0=60^\circ$. For $\varphi_0=30^\circ$, the reactance remains zero for most of the interval, and for $\varphi_0=45^\circ$, the reactance is only slightly below zero. At the end of the interval [0, 0.66λ], the curve is undefined (it becomes infinite) for $\varphi_0=60^\circ$.

Figures 4(a) and **(b)** show the dependence of $H_z(x)$, normalized relative to the field $H_{z0}(x)$ above an ideal conducting plane for fixed $h=0.5\lambda$ and various angles:

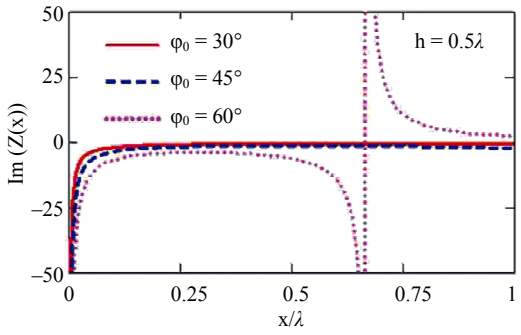

Figure 3. Variation of impedance distribution relative to Equation (8) for fixed $h = 0.5\lambda$ and different angles: $\varphi_0 = 30^\circ$ (solid line), $\varphi_0 = 45^\circ$ (dashed line) and $\varphi_0 = 60^\circ$ (dotted line). The length of the structure is $L = \lambda$. The impedance distribution which gives a reactance with a nearly hyperbolic character is the one for the angle $\varphi_0 = 60^\circ$.

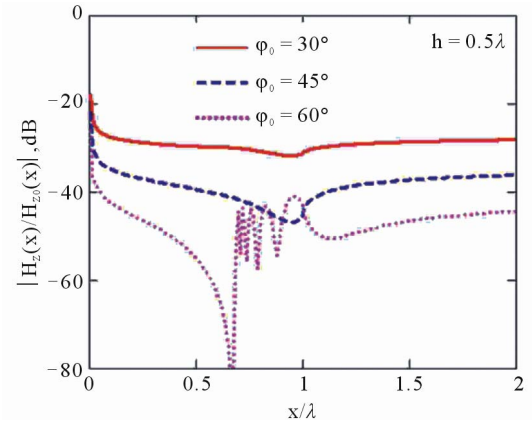

(a)

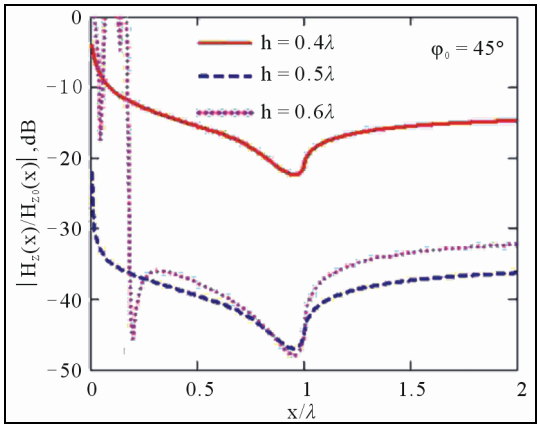

(b)

Figure 4. (a) Behavior of the complete field along the structure for fixed $h = 0.5\lambda$ and various angles: $\varphi_0 = 30^\circ$ (solid line), $\varphi_0 = 45^\circ$ (dashed line) and $\varphi_0 = 60^\circ$ (dotted line); (b) Behavior of the complete field along the structure for $\varphi_0 = 45^\circ$ and $h = 0.4\lambda$ (solid line); $h = 0.5\lambda$ (dashed line) and $h = 0.6\lambda$ (dotted line). The length of the structure is $L = \lambda$ for both cases. The largest decoupling level is obtained with the parameters: $\varphi_0 = 60^\circ$ and $h = 0.5\lambda$.

$\varphi_0 = 30^\circ$ (solid line), $\varphi_0 = 45^\circ$ (dashed line) and $\varphi_0 = 60^\circ$ (dotted line); and for the fixed angle $\varphi_0 = 45^\circ$ with various values of the parameter, $h = 0.4\lambda$ (solid line), $h = 0.5\lambda$ (dashed line) and $h = 0.6\lambda$ (dotted line), respectively. The length of the impedance structure is equal to $L = \lambda$ for both cases. The results of calculations show that the best data (greatest decoupling) are obtained with the parameters h and φ_0 when the impedance acquires the greatest capacitive value near the source of radiation. The greatest decoupling level is obtained with $\varphi_0 = 60^\circ$ and $h = 0.5\lambda$. The synthesized impedance which gives appropriate results for increased decoupling should be taken into account, because it has a large negative value of the reactive part in close proximity to the antenna. This leads to the fact that the impedance practically creates an anti-phase field relative to the ideal conducting surface. As a result, all the energy of the electromagnetic field transfers into the energy stored around the antenna. The structure turns into a resonator without losses (for the reactive impedance), including radiation. As an example, **Figure 5** shows the radiation patterns $F(\varphi) = \frac{k}{2}\int_0^L E_x(x')e^{ikx'\cos\varphi}dx'$ of the antenna located above the ideal conducting surface (dashed line) and the impedance surface (solid line) with the parameters: $\varphi_0 = 60^\circ$ and $h = 0.5\lambda$. From the graph, it is apparent that decoupling is provided with reduction of the radiation field by 35 dB; *i.e.*, a reduction of the main lobe of the radiation pattern.

Figure 6 shows the variation of the impedance distribution relative to Equation (11). The resulting impedance distribution is nearly flat (crossing zero at $x = 0.25\lambda$ and $x = 0.75\lambda$), except for a sharp Fano-type variation at $x = 0.5\lambda$. The reactance reaches its minimum point with a capacitive reactance of 60, and sharply transitions to a maximum inductive value of 60. The behavior of the complete field along the structure relative to **Figure 6** is also shown in **Figure 7** where the normalized impedance at point $x = 0$ acquires a value close to 500. The dash-dotted line shows this case. The dashed and solid lines correspond to the limiting maximum impedance values of 100 and 50, respectively. The dotted curve shows the case with negative impedance limited to the value –50. As we can see, field reduction in this case surpasses all the rest. It is evident that the main factor in increasing the decoupling is not the variation of the impedance distribution, but its limiting value near the antenna. This value leads to the appearance of an anti-phase reflected field, *i.e.*, to a sharp reduction of the radiation field. At the same time, research into the behavior of the complete field along the impedance structure in **Figures 4** and **7** shows that behind the structure on the region of the surface with zero impedance, the intensity of the magnetic field $H_z(x)$ sharply increases like the behavior of the field above an inhomogeneous reactance. Analogous phenomena are considered on all regions where the value of the reactance approaches zero or

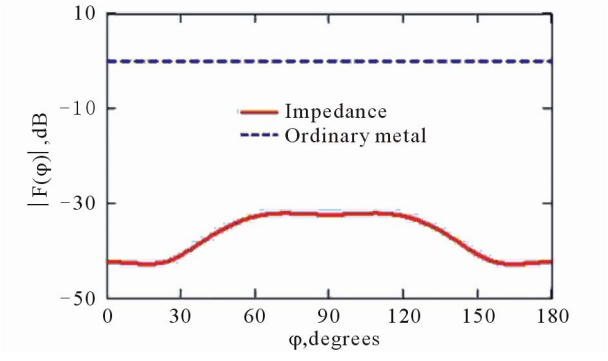

Figure 5. Radiation patterns of the antenna located above the ideal conducting (dashed line at 0 dB) and impedance (solid line) surfaces. The parameters for the calculation are: $\varphi_0 = 60^\circ$ and $h = 0.5\lambda$. The graph shows that the decoupling is provided with reduction of the radiation field by 35 dB for the main lobe of the radiation pattern.

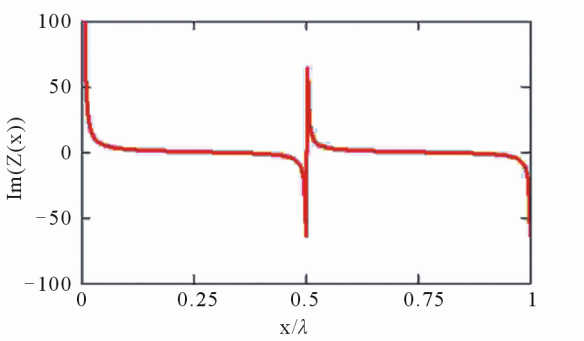

Figure 6. Variation of the impedance distribution relative to Equation (11).

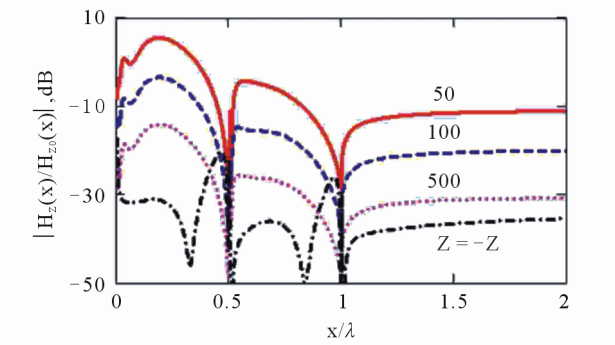

Figure 7. Variation of the complete field along the structure relative to the impedance distribution obtained in Figure 6. The dash-dotted curve is the case when the limiting value of the maximum impedance is 500. The dashed and solid curves correspond to limiting values of 100 and 50, respectively. The dotted curve shows the case with negative impedance limited to the value –50. The field reduction for the negative impedance gives the best results.

acquires positive values. Let us note that in **Figure 7**, the resulting field distributions have oscillatory behavior.

Next, we consider the possibility of designing decoupling structures on the basis of the impedance structure synthesized above, *i.e.*, taking into account the aperture of the receiving antenna. **Figure 8** shows the distribution of the complete field normalized to the amplitude of the path wave of the radiator in the openings of waveguide antennas $(a = b = 0.34\lambda)$ and along the structure $L = \lambda$ for the impedance calculated by Equation (8) for the parameters, $h = 0.5\lambda$ and $\varphi_0 = 30^\circ$ (dashed line) ($K = -31$ dB, the coefficient of standing waves (CSW) CSW = 2.37); $\varphi_0 = 45^\circ$ (dotted line) ($K = -34.6$ dB, CSW = 2.32); $\varphi_0 = 60^\circ$ (dash-dotted line) ($K = -40$ dB, CSW = 2.36). The solid line corresponds to the ideal conducting structure. As we can see, the angle, $\varphi_0 = 60^\circ$, which provides a higher level of decoupling, has a large CSW value of 2.36, because of large capacitive reactance near to the antenna opening. Such a structure is of a little use for near-omnidirectional transmitting antennas. In order to decrease the CSW, it is necessary to move the impedance structure aside from the antenna opening so that there is zero or low inductive reactance near the opening. On the other hand, the CSW is better when the angle is $\varphi_0 = 45^\circ$. Unfortunately, in this case, the coefficient of decoupling is smaller. It is important to note that in the presence of the ideal conducting surface, the weakening of the field is half as large during coupling along the geodesic line.

Distribution of the impedance for the structure which provides the greatest decoupling is shown in **Figures 9(a)** $(L = \lambda)$ and **(b)** $(L = 2\lambda)$. The dimensions $a = b = 0.34\lambda$ are similar for both cases. The resulting impedance distributions are parabolic in some small intervals. As in **Figure 3**, they don't have any points at the

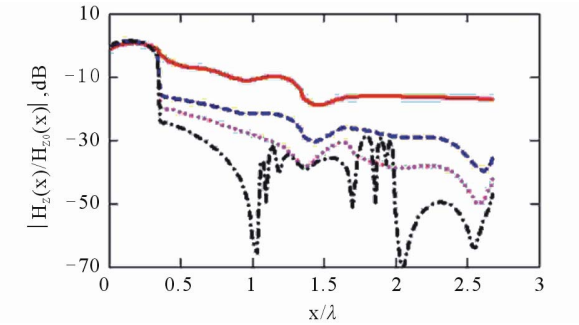

Figure 8. Distribution of the complete field for the impedance calculated by Equation (8) for the parameters, $a = b = 0.34\lambda$, $h = 0.5\lambda$ and $\varphi_0 = 30^\circ$ (dashed line, *CSW* = 2.37); $\varphi_0 = 45^\circ$ (dotted line, *CSW* = 2.32); $\varphi_0 = 60^\circ$ (dash-dotted line, *CSW* = 2.36). The solid line corresponds to the case of an ideal conducting surface. As is evident, the angle, $\varphi_0 = 60^\circ$, which provides a better level of decoupling has a large CSW value of 2.36, due to a large capacitive reactance near to the antenna opening.

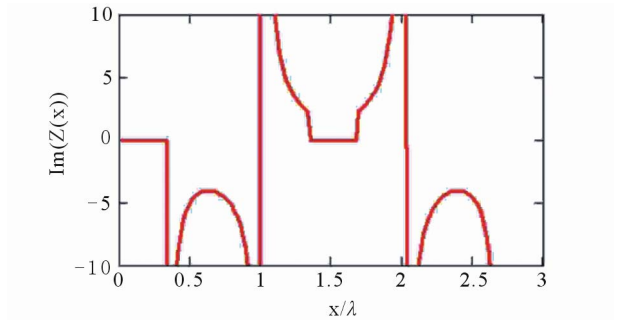

(a)

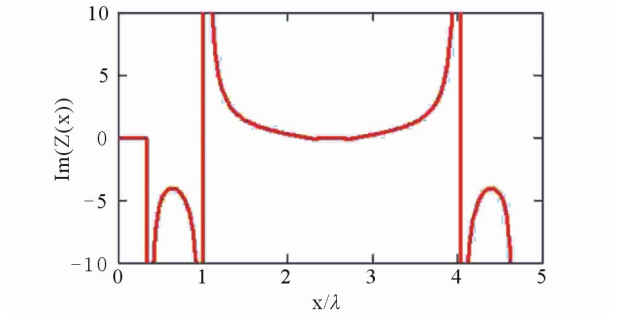

(b)

Figure 9. (a) Distribution of the impedance for the structure which provides the greatest decoupling for the parameters, $h = 0.5\lambda$, $\varphi_0 = 60^\circ$ and $L = \lambda$; (b) The same distribution is also presented for these parameters, but with $L = 2\lambda$. The dimensions $a = b = 0.34\lambda$ are similar for both cases. The resulting impedance distributions are parabolic in some small intervals.

extremities and outside of the interval. As we can see, increasing the size of the structure to $L = 2\lambda$ only doubled the scale of the positive value of the reactance, without changing the character of its distribution. The value of the field in the opening of the receiving antenna (**Figure 10**) has somewhat grown. However, the level of decoupling has nevertheless increased by 3 dB, becoming equal to 43.4 dB. To explain this fact, **Figure 11** shows the distributions of the real (solid line) and the imaginary (dashed line) components of the complete field. It is clear that both components of the field in the opening of the receiving antenna are very weak, and consequently, their impact on the main wave in the receiving antenna is not significant. In this connection, it is possible to state that there is no opportunity to completely characterize the degree of decoupling between antennas solely on the basis of the amplitude distribution of the field along the structure and in the openings of the antennas. During the designing of decoupling structures, it is necessary to also control the coefficient of decoupling $K = -10\log(K_c)$, where K_c is the coefficient of antenna coupling. We also note that, as in **Figure 7**, the distribution of the field in **Figure 10** has oscillating, non-monotonic behavior.

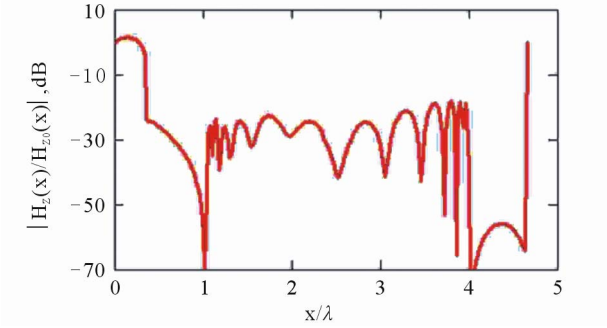

Figure 10. Distribution of the field relative to Figure 9(b). The resulting field distribution has oscillating, non-monotonic behavior.

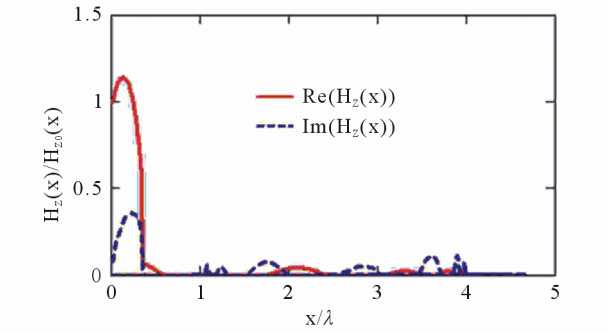

Figure 11. Distribution of the complete field relative to Figure 9(b), showing the real (solid line) and the imaginary (dashed line) components. It is clear that both components of the field in the opening of the receiving antenna are very weak.

Nevertheless, we can consider the results of antenna decoupling using the structure giving the impedance distribution presented in **Figure 12**, as calculated by Equation (11) for the same system parameters as in **Figure 8**. The resulting impedance distribution has a reactance close to the character of the tangent function. Beyond the receiving antenna, the impedance distribution is inverted. With this level of decoupling, this structure gives the same result ($K \approx -31$ dB) as in the previous case for the structure with the parameters: $h = 0.5\lambda$ and $\varphi_0 = 90^\circ$ (see **Figure 8**, solid line) shown in **Figure 13**. We note that **Figure 13** also has oscillating, non-monotonic behavior. Finally, we mention that the optimization of the impedance decoupling structures is ideally fulfilled not by the level of the field distributed along the synthesized structure (although this also gives some positive results), but by the level of decoupling K, or more exactly, by the level of the main wave H_0^{rec} in the receiving antenna.

5. Conclusions

In summary, we have solved the problem of designing a heterogeneous impedance plane given a stated reflected

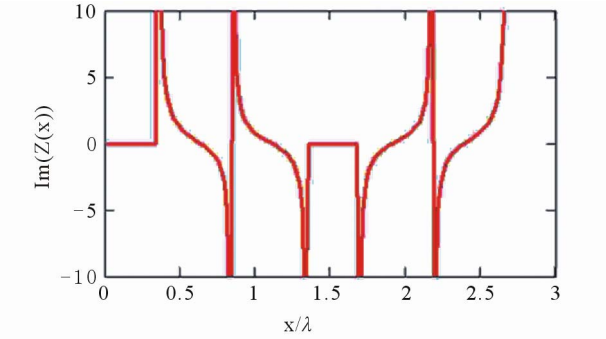

Figure 12. Variation of the impedance calculated by Equation (11). The parameters for our calculation are $a = b = 0.34\lambda$, $L = \lambda$, $h = 0.5\lambda$ and $\varphi_0 = 60^\circ$. The resulting impedance distribution has a reactance close to the character of the tangent function. Beyond the receiving antenna, the impedance distribution is inverted.

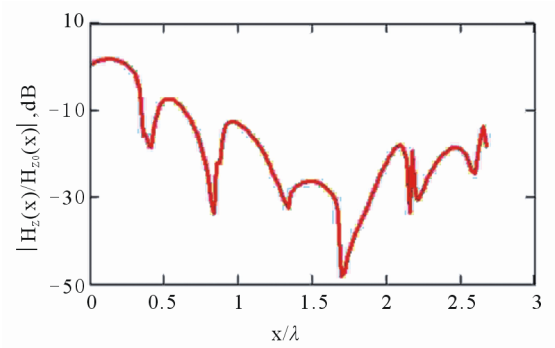

Figure 13. Distribution of the complete field relative to Figure 12. The parameters for our calculation are the same as in Figure 8. The resulting field distribution has oscillating, non-monotonic behavior.

field. We obtained the variation of the impedance distribution of the purely reactive surface in explicit form. The calculations show that the best results are given by the parameters, $\varphi_0 = 60^\circ$ and $h = 0.5\lambda$, for which the impedance acquires large capacitive values near the source of radiation. However, during the solution of the design problem, the interaction between antennas was not taken into account. It is evident that the presence of the receiving aperture antenna will lead to unwanted reduction of antenna decoupling by means of the heterogeneous features created by the very aperture of the receiving antenna.

Taking into account the receiving antenna, we found a solution to the problem of analysis of the EMF of two waveguides antennas located on the same impedance plane on the basis of the impedance designed in Section 2. The calculated result has shown that to limit coupling between antennas, we need to take into consideration both the amplitude distribution of the field along the structure and in the openings of the antennas. Moreover, during the designing of the structure, it is necessary to

also control the coefficient of decoupling.

REFERENCES

[1] K. G. Klimachev, "Fundamentals of Forecasting and Provision of Electromagnetic Compatibility of Radio Engineering Systems and Devices," Moscow Aviation Institute, Moscow, 1994.

[2] A. I. Sapgira, "Electromagnetic Compatibility of Radio Electronic Devises and Unpredicted Interferences, Vol 1: General Questions of EMC," Soviet Radio, Moscow, 1977.

[3] N. C. Karmakar and M. N. Mollah, "Potential Applications of PBG Engineered Structures in Microwave Engineering: Part I," *Microwave Journal*, Vol. 47, No. 7, 2004, pp. 22-44.

[4] P. S. Kildal, "Artificially Soft and Hard Surfaces in Electromagnetics," *IEEE Transactions on Antennas and Propagation*, Vol. 38, No. 10, 1990, pp. 1537-1544. doi:10.1109/8.59765

[5] P. S. Kildal, A. A. Kishk and A. Tengs, "Reduction of Forward Scattering from Cylindrical Objects Using Hard Surfaces," *IEEE Transactions on Antennas and Propagation*, Vol. 38, No. 10, 1990, pp. 1537-1544. doi:10.1109/8.59765

[6] R. E. Lawrie, "The Control of the Echo Area of Ogives by Cutoff Corrugated Surfaces," *IEEE Transactions on Antennas and Propagation*, Vol. 14, No. 6, 1966, pp. 798-799. doi:10.1109/TAP.1966.1138802

[7] J. Carlsson and P. S. Kildal, "Transmission through Corrugated Slots," *IEEE Transactions on Electromagnetic Compatibility*, Vol. 37, No. 1, 1995, pp. 114-121. doi:10.1109/15.350251

[8] R. B. Hwang and S. T. Peng, "Surface-Wave Suppression of Resonance-Type Periodic Structures," *IEEE Transactions on Antennas and Propagation*, Vol. 51, No. 6, 2003, pp. 1221-1229. doi:10.1109/TAP.2003.811470

[9] G. Goussetis, A. P. Feresidis and P. Kosmas, "Efficient Analysis, Design, and Filter Applications of EBG Waveguide with Periodic Resonant Loads," *IEEE Transactions on Microwave Theory and Techniques*, Vol. 54, No. 11, 2006, pp. 38853892. doi:10.1109/TMTT.2006.883648

[10] Y. S. Joe, J.-F. D. Essiben, E. R. Hedin, J. T. N. Bisse and J. Matanga, "Optimization of Impedance Plane Reducing Coupling between Antennas," *Wireless Engineering and Technology Journal*, Vol. 2, No. 1, pp. 1-8, 2010. doi:10.4236/wet.2011.21001

[11] Yu. V. Yukhanov, "Analysis and Synthesis of Impedance Plane," *Radiotechnics and Electronics*, Vol. 45, No. 4, 2000, pp. 404-409.

[12] A. Yu. Yukhanov, "Synthesis of Reactance Anisotropic Plane Excited By a Thread of In-Phase Magnetic Current," *International Conference on Radiation and Scattering of Electromagnetic Waves*, Taganrog, 20-25 June 2005, pp. 360-362.

[13] A. Yu. Yukhanov, "Two-Dimensional Task of Impedance Plane Synthesis," *Radio Engineering Circuits*, *Signals and Devices*, Vol. 45, 1998, pp. 92-95.

[14] Y. S. Joe, J-F. D. Essiben and E. M. Cooney, "Radiation Characteristics of Waveguide Antennas Located on the Same Impedance Plane," *Journal of Physics D*: *Applied Physics*, Vol. 41, No. 12, 2008, Article ID: 125503. doi:10.1088/0022-3727/41/12/125503

[15] O. N. Tereshin, V. M. Sedov and A. F. Chaplin, "Synthesis of Antennas on Decelerating Structures," Communication Press, Moscow, 1980.

